CAD-Based Range Sensor Placement for Optimum 3D Data Acquisition

F. Prieto[1,3], T. Redarce[1], P. Boulanger[2] and R. Lepage[3]

[1] INSA, Laboratoire d'Automatique Industrielle,
20 avenue Albert Einstein, 69621 Villeurbanne Cedex, France, {fprieto, redarce}@lai.insa-lyon.fr
[2] NRCC, Institute for Information Technology, Montreal road, building M-50
Ottawa, Ontario, K1A 0R6, Canada, boulanger@iit.nrc.ca
[3] ÉTS, Laboratoire d'Imagerie, de Vision et d'Intelligence Artificielle,
1100 rue Notre-Dame Ouest, Montréal, Québec, H3C 1K3, Canada, lepage@livia.etsmtl.ca

Abstract

The use of laser range sensor allows very significant improvement in acquisition speed but does not equal the accuracy obtained with a coordinate measuring machine. In order to obtain a quality control close to that obtained in metrology, we suggest to improve the accuracy of the depth measurements by positioning the sensor's head according to a strategy for optimum 3D data acquisition. We propose in this paper such a strategy to automatically produce a sensing plan for completely and accurately acquiring the geometry of a surface or of the whole piece whenever possible. The system requires the exact position and orientation of the part and its CAD model in IGES format. There is no limitation regarding the shape of the part to be digitized. An auto-synchronized range sensor developed at the NRCC was used, and for this sensor, the accuracy of the 3D measured points is a function of the distance and of the incident angle relative to the surface. Our strategy guaranties that the viewpoints found meet the best accuracy conditions in the scanning process.

1. Introduction

Automatic inspection using range sensor is a complex task that requires an exact geometrical definition of the part and a large number of measurement points. The use of coordinate measuring machine and recent progress in laser sensors combining measurement accuracy and fast acquisition speed allow one to obtain many accurate 3D measurements. These 3D points form an explicit description of object surface. In addition, knowledge of the corresponding CAD model provides an exact and complete description of the geometry of the object under inspection. We have developed a method for automatic inspection of parts containing complex surfaces. The system use CAD model (in IGES format) and 3D data provided by a telemetric sensor fixed to a coordinate measuring machine (CMM). The quality of the results depends almost exclusively on the accuracy of measurements.

At present, it is near to impossible to compare the accuracy obtained with a CMM equipped with a contact sensor (lower than the micron) and those delivered by a CMM equipped with a laser range finder (about 25 micron at best). If one wants to take advantage from the speed of acquisition obtained with a range sensor to make systematic dimensional check of complex parts, it is necessary to attain the best possible accuracy of the depth images obtained with a range sensor.

The 3D sensors, delivering information on the surface of the object, all operate generally according to a common principle: emission of a laser beam (incidental ray), usually from a laser diode, followed by the analysis of the reflected ray [9], [10]. From this analysis, we obtain the spatial position of each point (x, y, z), relative to the reference frame of the sensor, and also for certain sensors the luminance information. The optics laws dictate that the laser ray be normal to the surface for maximum reflected energy.

In order to meet this constraint of perpendicularity, we propose digitizing the object by following strategies aiming to keep the laser beam as normal as possible to the queried surface. Moreover, the sensor used to carry out our experiments have the property of increased accuracy when it is closer to the object, the minimal distance corresponding to its depth of field. Therefore, we have developed a constrained digitalization technique allowing on one hand to keep the sensor as normal as possible to the surface, while obeying a criterion of accuracy defined by the operator and chosen to avoid occlusions. We modeled the accuracy of the

sensor as a function proportional to the distance between the sensor and the surface and to the incident angle. Using this model, we can constraint the scanning process to produce a set of 3D points with a predefined accuracy.

We propose in this paper an acquisition planning strategy based on *a priori* knowledge of the object supplied by the CAD model.

2. Related literature

The problem of sensor planning in computer vision is addressed by Tarabanis *et al* [11] as following: for a given information concerning the environment (object under observation, sensor available) and concerning the task that the system must achieve (detection of characteristics, object recognition, scene reconstruction), to develop some automatic strategy to determine the sensor parameters (the position, the orientation and the optical parameters of the sensor) to carry out the task satisfying some criteria. The majority of work carried out in the field of sensor position planning is mainly to find the best views to digitize an object without missing zones, and with a minimum number of views. It is usually considered that the environment is unknown, that no information on the type of object is known, neither its position nor its orientation. In [11], Tarabanis *et al* survey the problem of sensor planning in computer vision and tackled it from the point of view of acquiring depth images (3D) and luminance ones (2D). In the case of 2D images alone, one can refer to the work of Cowan and Kovesi [2], Ben Amar *et al* [1] and Redarce *et al* [8].

Tarabanis *et al* [12] developed a model-based sensor planning system. The Machine Vision Planner (MVP) automatically computes vision sensor parameter values that satisfy several sensor constraints such as detectability, visibility and field of view. Inputs to the MVP model are: the object geometric information from a CAD database as well as models of camera and lens. Outputs are the camera position and setting values for which features of interest of polyhedral objects are visible, contained entirely in the sensor field of view, in focus and resolvable by the given specifications of the sensor. This system works with 2D image obtained from a CCD camera.

Truco *et al* [5], [4], reported a general automatic sensor planning system (GASP) designed to compute optimal positions for inspection tasks, using a known imaging sensor (like a 3D range sensor) and feature-based object models. GASP exploits a feature inspection representation (FIR) which outputs off-line the explicit solution for the sensor-positioning problem. Viewpoint is defined optimally as a function of feature visibility and measurement reliability. GASP computes visibility with an approximate model; the reliability of inspection depends on the physical sensors used and on the processing software. Truco *et al* demonstrate a complete inspection session involving 3D object positioning, optimal sensor position, and feature measurement from the optimal viewpoint.

Newman *et al* [19] developed a system that can detect defects of castings using range images. This system uses CAD model information for surface classification and inspection. Authors assert there are several advantages for the use of range images in inspection, For example: the accuracy of depth measurement and the insensitivity to ambient light; these advantages allow objects to be extracted more easily from their background, and most important, range images explicitly represent surface information. The authors show the interest for the use of the CAD model in order to carry out the control task. Moreover, they show the weakness of the current CAD systems to make automatic check.

In the previous works, the placement strategy is optimized to have the minimum number of viewpoints that digitized the whole part. In our work, the placement strategy optimizes the accuracy of the acquired 3D points and can be applied to a particular surface or to the whole part.

Some interesting works that deal with the reconstruction problem are those by Pito [18], [17] and by Papadopoulos and Schmitt [3]. Pito presents a solution for the next best view problem (NBV) of a depth camera in the process of digitizing unknown parts. The system builds a surface model by incrementally adding range data to a partial model until the entire object has been scanned. No assumptions are made about the geometry or topology of the object. Papadopoulos proposes an automatic method for digitizing unknown 3D parts using an active sensor with a small field of view. Because of their small field of view, the sensor navigates closely to the object and is subject to collisions, so a special algorithm is proposed to avoid collisions.

We have worked for several years on measurement control by registration of CAD models and range images [20], [7]. We showed that the size of the defects that can be detected depends in a very significant way on the sensor accuracy. Therefore in this work, we seek to improve the 3D data accuracy by using strategies in the acquisition process.

3. The 3D range camera

This section describes the optical principle of the range camera used and the accuracy of the 3D data as a function of the camera placement. The camera, an auto-synchronized range sensor, was developed at National Research Council of Canada [6].

3.1. Optical principle

The basic geometry of the NRCC 3D laser camera is based on the synchronization of the projected laser beam with its return path. The main advantage of this approach is

to simultaneously obtain high resolution and large field of view contrary to standard triangulation geometries where a compromise is made between resolution and field of view [13], [15], [14].

The synchronized scanning geometry is based on a doubled-sided mirror used to project and detect a focused or collimated laser beam (Figure 1).

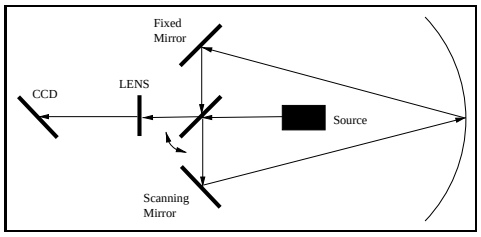

Figure 1. Optical setup of the NRCC range sensor.

The scanning of the target surface by the sensor results in the output of 3D points (x, y, z) and their luminous intensity (I) at the surface. The auto-synchronized sensor explores surface line by line at a rate that can be specified by the user (usually 512 points/line). The resolution is a function of the length of this line, and therefore of the distance separating the sensor from the object. The sensor is mounted on a Coordinate Measuring Machine (CMM) to allow precise mechanical registration between views, and to place the camera in the desired location. The result of the digitalization is an unordered series of measurements describing the scanned object's surface.

3.2. Accuracy of the sensor

In order to evaluate the accuracy of the 3D points cloud obtained by the scanning process, we have achieved 128 measurements in different positions for distance and orientation of the laser sensor with respect to a reference surface. The measurements were fulfilled after the camera calibration process, and the camera placements were near to calibration ones. In a first experiment, we averaged up to 256 measurements of a same 3D point and converge toward a constant mean value within 64 measurements, so we take 128 measurements to compute the variance at each point.

In Figure 2, we show the variance (in mm^2) in the axis of the projected beam versus the distance (in mm) from the camera to the surface. The continuous curve is a second degree polynomial that best fit the real variances curve. The fitting curve is defined by $Var(d) = 6\text{E-}10d^2 - 2.22\text{E-}7d + 2.416\text{E-}5$. From Figure 2, we can conclude that in spite of oscillations, the variance has a smaller dispersion when the camera is the near to the surface. Since the goal of this work is improve the measurement accuracy by finding the best scanning placements, we define a distance range for the placements as $170mm \leq d \leq 240mm$.

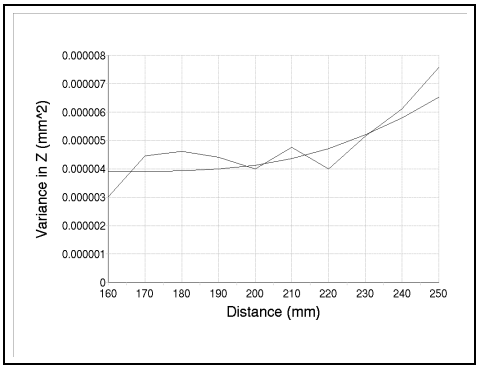

Figure 2. Variance in Z versus distance.

In Figure 3, we show the variance (in mm^2) in the laser propagation axis versus the incident angle (in degrees) the laser beam reaches the surface. The continuous curve is an exponential function $Var(\alpha) = 3\text{E-}6e^{0.07\alpha}$ that best fit the real curve of variances. The incident angle is measured in the same direction as the laser beam sweep. From Figure 3, we observed that the smaller value of dispersion is produced for an incident angle near to zero degrees, or normal to the surface. For the definition of the best scanning placements, we set the laser beam sweep range as $-35^\circ \leq \alpha \leq 35^\circ$. The range starts at -35° and not 0° because we have a symmetrical result when the angle α increases in the opposite direction.

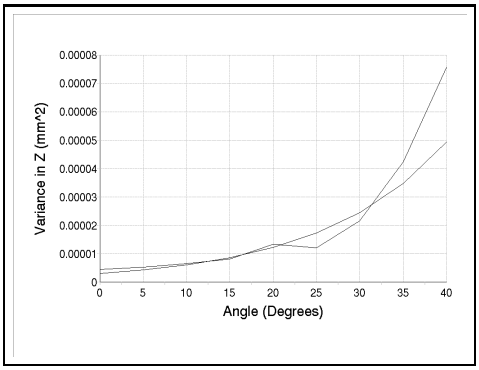

Figure 3. Variance in Z versus incident angle in the direction of the laser sweep.

Another parameter which influence the value of the variance is the incident angle in a perpendicular direction from the laser beam sweep (angle (β)). In Figure 4, we present the variance (in mm^2) in the axis of the beam projection

versus the incident angle β (in degrees). The continuous curve is an exponential function $Var(\alpha) = 4\text{E-}6e^{0.0415\alpha}$, the best fit of the real variance curve. Similarly as for the angle α, we can conclude from Figure 4 that the dispersion is smaller when the incident angle is near to zero, or normal to the surface. For the definition of the best scanning placements, and looking at the behavior of the curve we have set the laser beam sweep range as $-35° \leq \beta \leq 35°$.

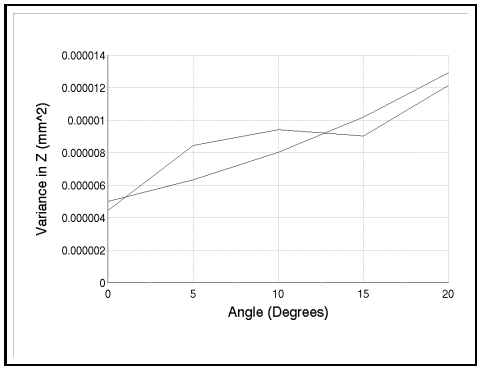

Figure 4. Variance in Z versus incident angle in a perpendicular direction to the laser sweep.

These results confirm that we can improve the accuracy of the data acquisition process by following the previously defined criterions (normal direction, distance). So, in order to be able to achieve inspection tasks, we have implemented an acquisition planning strategy. The strategy improve the 3D data accuracy by finding the optimal camera placement for digitizing the part, using the range of the parameters d, α and β computed in this section. The acquisition planning strategy is explained next.

4. An optimum 3D data acquisition strategy

The main goal of this work is to improve the measurement accuracy of a part with the aid of a sensor placement strategy. Such a strategy consists in computing the set X of viewpoints x^i in order to obtain a complete and optimal 3D image of the part. We define an optimal 3D image as a 3D cloud acquired by the scanning process in the best accuracy conditions. The resulting 3D image can be used, for instance, in inspection task for verifying the specification of just a few surfaces. Our strategy is therefore to find the collection of viewpoints for each surface independently. If one wants to digitize the whole part, he just has to add the complete assemblies X of all the surfaces in the part.

We define a viewpoint as a set of 7 parameters $x^i = \{x, y, z, \phi, \theta, \psi, \gamma\}^i$, with three position parameters (x, y, z) defining the spatial placement of the camera relative to the coordinate system of the part, three orientation parameters (ϕ, θ, ψ) defining the direction of the laser beam, and one parameter γ specifying the angle of the controlled sweep. Figure 5 shows a viewpoint with all its parameters. We do not consider optical parameters because the laser camera is previously calibrated. The set X of viewpoints x^i is defined $X = \{x^1 x^2 ... x^i ... x^n\}$, with n the minimum number of viewpoints to digitize a simple surface or the whole part.

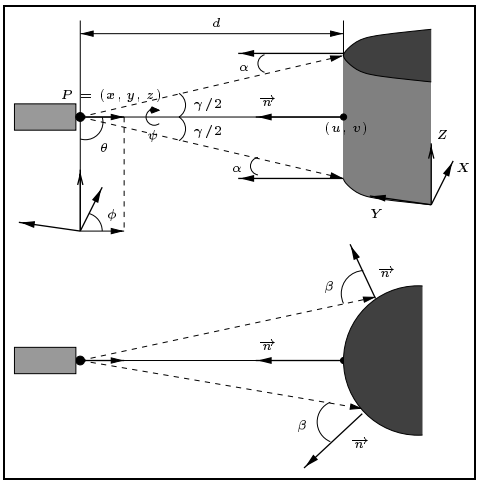

Figure 5. Viewpoint parameters.

The system requirements are: knowledge of the exact position and orientation of the part and the CAD model of the part in IGES format. We use a registration process to determine the placement of the part, as implemented by Moron [20] and which relies on the well-known work of Besl and McKay [16]. This process registers an unordered cloud of 3D points of the part with its CAD model. The CAD model is used not only for the registration process, but also for the search of viewpoints and to resolve the occlusion problem.

From the last section, we showed that the accuracy of a measured point using an auto-synchronized range sensor (previously calibrated) depends specifically on the scanning distance and on the incidence angle of the laser beam relative to the surface. We have found for the auto-synchronized range sensor that the near and far field view planes are $170mm$ and $240mm$ respectively. The measured points are therefore more accurate when the camera is located near the part. For the best accuracy, the ideal incident angle the laser beam reaches the surface is 90 degrees ($\alpha = 0$ and $\beta = 0$ see Figure 5), that is the more the angle of incidence of the laser ray is near to the normal direction of the surface, the more the measured points are accurate. Our strategy searches for viewpoints to digitize the part with the best conditions for accuracy.

The viewpoint issue of our strategy is that inspected surface can be reached by the camera mechanical support and is occlusion free. A surface is occluded for a specific viewpoint if any object intersects the laser beam before reaching the target surface. The system works with both simple and complex surfaces. The only geometric constraint imposed to the parts to be digitized is that they are completely contained in the workspace of the camera.

The algorithm's pseudocode implemented as a solution to this problem is:

3D data acquisition strategy algorithm

1. *Input data.*
   - 1.1. *Extract data from the CAD model.*
   - 1.2. *Generate the 3D voxel model.*
2. *Find the viewpoints set.*
   - 2.1. *Project viewpoints on the surface.*
   - 2.2. *Find the optimal viewpoint placement.*
   - 2.3. *Verify the reachability and the non-occlusion conditions.*
3. *Estimate 3D data accuracy.*

4.1. Input data

Two processes basically generate the input data required for the algorithm. A first process extracts from the CAD file the needed data to search for viewpoint on the surfaces. The second process generates a 3D voxel model of the part.

CAD model. A CAD model of the part in IGES format is input to the algorithm. The IGES file contains the exact representation of the part using NURBS (Non-Uniform Rational B-Splines) surfaces parameters. A NURBS surface of order p in the parametric direction u and of order q in the parametric direction v is defined by the following equation:

$$\vec{s}(u,v) = \frac{\sum_{i=0}^{n}\sum_{j=0}^{m} N_{i,p}(u)N_{j,q}(v)w_{i,j}\vec{P}_{i,j}}{\sum_{i=0}^{n}\sum_{j=0}^{m} N_{i,p}(u)N_{j,q}(v)w_{i,j}}$$

with n and m the number of control points in the parametric direction u and v respectively, $\vec{P}_{i,j}$ the control points, $w_{i,j}$ the weight associated to the control point $\vec{P}_{i,j}$, $N_{i,p}$ (or $N_{j,q}$) the B-Spline base functions defined by the following recurrent formula:
$N_{i,p}(u) = \frac{u-u_{i-1}}{u_{i+p-1}-u_{i-1}}N_{i,p-1}(u) + \frac{u_{i+p}-u}{u_{i+p}-u_i}N_{i+1,p-1}(u)$ and
$N_{i,0}(u) = \begin{cases} 1 & \text{if } u_{i-1} \le u \le u_i \\ 0 & \text{elsewhere} \end{cases}$, where u_i, v_j are the inner knots belonging to the knot vectors of the NURBS surface, $u_i \in [u_0, u_1]$ and $v_j \in [v_0, v_1]$.

3D voxel model. Let $P(u,v)$ be a 3D surface representation of a part, defined by the union of its N parametric surface:

$$\begin{aligned} P(u,v) &= \sum_{i=1}^{N} \vec{s}_i(u,v) \\ &= \sum_{i=1}^{N} (S_{ix}(u,v), S_{iy}(u,v), S_{iz}(u,v)) \\ &= \sum_{i=1}^{N} (X_i(u,v), Y_i(u,v), Z_i(u,v)) = P(x,y,z) \end{aligned}$$

Let $P_D(x,y,z)$ be the *3D voxel model* of the part $P(u,v)$, and defined as:

$$\begin{aligned} P_D(x,y,z) = & \\ & \sum_{i=1}^{N}\sum_{j=0}^{Nu_i}\sum_{k=0}^{Nv_i} (Inf(X_i(u_i + j\Delta u_i, v_i + k\Delta v_i)), \\ & \qquad Inf(Y_i(u_i + j\Delta u_i, v_i + k\Delta v_i)), \\ & \qquad Inf(Z_i(u_i + j\Delta u_i, v_i + k\Delta v_i))) \\ & = \sum_{i=1}^{N}\sum_{j=0}^{Nu_i}\sum_{k=0}^{Nv_i} (X_{ijk}, Y_{ijk}, Z_{ijk}) \\ & = \sum_{i=1}^{N}\sum_{j=0}^{Nu_i}\sum_{k=0}^{Nv_i} V_{ijk} \end{aligned}$$

where $Inf(X(u,v))$ is the biggest integer inferior or equal to $X(u,v)$, and $\Delta u_i = \frac{u_{i1}-u_{i0}}{Nu_i}$ and $\Delta v_i = \frac{v_{i1}-v_{i0}}{Nv_i}$, with Nu_i and Nv_i two thresholds that guarantee that all *voxel* touched by the surface $\vec{s}_i$ is identified. The point (x,y,z) is defined by the *voxel* V_{ijk} as: $x_{ijk} \le x < x_{ijk} + 1$, $y_{ijk} \le y < y_{ijk} + 1$ and $z_{ijk} \le z < z_{ijk} + 1$. If we extend the concept of a two-dimensional binary bitmap, where each pixel (r,s) can take just one of two values, each voxel (i,j,k) in the 3D space can take one of two values: 0 (unoccupied) or 1 (occupied). An occupied voxel contains some portion of any of the surfaces that make up the part. The *3D voxel model* P_D is the addition of all occupied voxels. Clearly, $P(x,y,z) \subseteq P_D(x,y,z)$. The importance of this *3D voxel model* in the solution of the occlusion problem will be clarified later.

4.2. Search for the viewpoints set

We now describe how the NURBS surface parameters from the CAD model are used to search the viewpoints and to solve the occlusion and collision problem. We first generate a 2D bitmap of each surface to find the viewpoints projection on the surface. Then, the optimal placement for the viewpoint is computed using the normal direction of the

surface to each projected viewpoint. Finally, the occlusion and collision problems are solved by using the *3D voxel model*.

Viewpoints projection on the surface. We look for the set of projected viewpoints that define the trajectory that the camera mechanical support (a CMM in this work) has to follow in order to digitize the whole surface. The laser sweeping ray orientation has to be perpendicular to this trajectory to guarantee the minimal sweep distance from the trajectory to the edges of the surface. The area of surface to be digitized between two specific viewpoints depends on the distance d, of the field of view γ of the camera and on the distance between the two projected viewpoints. In most case the field of view γ is fixed and is set to 16 degrees for the range sensor used in this work. The distance d is a parameter computed according to the acquisition strategy, and is constrained between $170mm$ and $240mm$. The distance between the two projected viewpoints is set by the acquisition strategy. In fact, the portion of surface digitized from a specified viewpoint is defined by the rectangle $R = a \cdot b$, where a is the line formed by the laser ray projection on the surface and equals to $a = 2 \cdot d \cdot tan(\gamma/2)$, and b is the distance between the two projected viewpoints. The movement between two adjacent points follows a line with a slower speed than the laser sweep speed.

From the exactly definition of a trimmed parametric surface in the NURBS CAD model, we create a 2D bitmap of the surface. Our algorithm uses this bitmap to define: the best laser sweeping ray orientation and the set of viewpoint projections on the surface. Initially, the best direction for the laser sweeping ray is found (sweep is specified by the scanner's field of view). The best direction is defined as the one where the variation of the incidence angle (of the laser ray on the surface) for a complete sweep is the smallest. This algorithm works with any kind of surfaces (simple or complex) so the selection of the best direction is a very important criterion. The Figure 6 shows the projected viewpoints trajectory found to digitize a cylindrical surface (the projected viewpoints trajectory is highlighted by an arrow). The incident angle for a complete sweep is larger for a horizontal sweep than for a vertical sweep. Because the laser sweep is perpendicular to its trajectory, we conclude that the found solution is the best one.

We are looking for the best viewpoint set to improve the accuracy of the 3D measurement points. The strategy searches for points such that the sweep distance up to the edges of the surface is similar and as short as possible. A larger sweep distance means either a greater angle of incidence or a too far away distance from the 3D camera to the surface. As the scanning process is more accurate when the sweep distance is shorter, the strategy looks for a trajectory with a symmetrical distance to the edges of the surface.

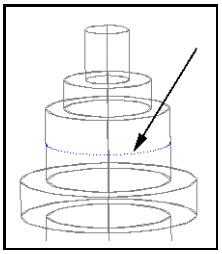

Figure 6. Projected viewpoint trajectory to digitize a cylindrical surface.

Figure 7 illustrates the solution found for flat surfaces.

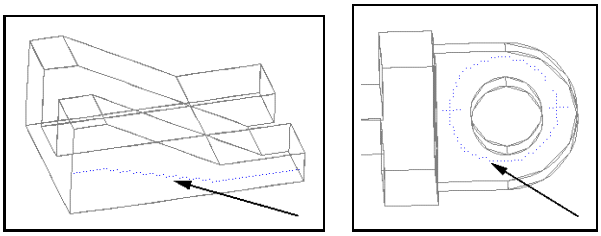

(a) (b)

Figure 7. Projected viewpoint trajectories with the smallest sweep distances involving flat surfaces.

Optimal viewpoint placement. To complete the definition of a viewpoint, we need to find its position and orientation in space. For that purpose, we compute the normal direction of the viewpoints obtained in the previous section. For a point (u, v), on the parametric surface $\vec{s}$, the normal direction is computed using:

$$\overrightarrow{n} = \frac{\frac{\partial}{\partial u}\vec{s}(u,v) \times \frac{\partial}{\partial v}\vec{s}(u,v)}{\| \frac{\partial}{\partial u}\vec{s}(u,v) \times \frac{\partial}{\partial v}\vec{s}(u,v) \|^2}$$

with $\frac{\partial}{\partial u}\vec{s}(u,v) = \frac{AB-CD}{B^2}$ and $\frac{\partial}{\partial v}\vec{s}(u,v) = \frac{EB-FD}{B^2}$ where

$$A = \sum_{i=0}^{n}\sum_{j=0}^{m}(\frac{\partial}{\partial u}N_{i,p}(u))N_{j,q}(v)w_{i,j}\vec{P}_{i,j},$$
$$B = \sum_{i=0}^{n}\sum_{j=0}^{m}N_{i,p}(u)N_{j,q}(v)w_{i,j},$$
$$C = \sum_{i=0}^{n}\sum_{j=0}^{m}N_{i,p}(u)N_{j,q}(v)w_{i,j}\vec{P}_{i,j},$$
$$D = \sum_{i=0}^{n}\sum_{j=0}^{m}(\frac{\partial}{\partial u}N_{i,p}(u))N_{j,q}(v)w_{i,j},$$
$$E = \sum_{i=0}^{n}\sum_{j=0}^{m}N_{i,p}(u)(\frac{\partial}{\partial v}N_{j,q}(v))w_{i,j}\vec{P}_{i,j},$$
$$F = \sum_{i=0}^{n}\sum_{j=0}^{m}N_{i,p}(u)(\frac{\partial}{\partial v}N_{j,q}(v))w_{i,j},$$

$$\frac{\partial}{\partial u}N_{i,p}(u) = \frac{p}{u_{i+p-1}-u_{i-1}}N_{i,p-1}(u) - \frac{p}{u_{i+p}-u_i}N_{i+1,p-1}(u) \quad \text{and}$$

$$\frac{\partial}{\partial v}N_{j,q}(v) = \frac{q}{u_{j+q-1}-u_{j-1}}N_{j,q-1}(v) - \frac{q}{u_{j+q}-u_j}N_{j+1,q-1}(v)$$

We know that the accuracy is a function of the distance and of the incident angle of the laser beam. For the same portion of surface to be digitized, there is a relation between the resolution of the scanning process and the amplitude of the incident angle at a fixed distance from the camera to the surface. For a far-off distance, the resolution will be lower but the incident angle will be smaller. From Figure 2, one can concludes that for an incident angle of $\pm 8^{\circ}$, the variation in the accuracy is similar to the variation when the distance is varied from $170mm$ and $240mm$ (see Figure 2). For an inspection task, it is important to have a large number of measurement points, meaning a high density scan. The viewpoint will then be placed as close as possible to the surface.

In Figure 8, we show the viewpoints found by using our strategy for two dissimilar parts. In Figure 8 (a), we illustrate the change in the orientation of the viewpoint when we digitize a complex surface. In Figure 8 (b), we illustrate the viewpoint distance variation as a function of the sweep distance.

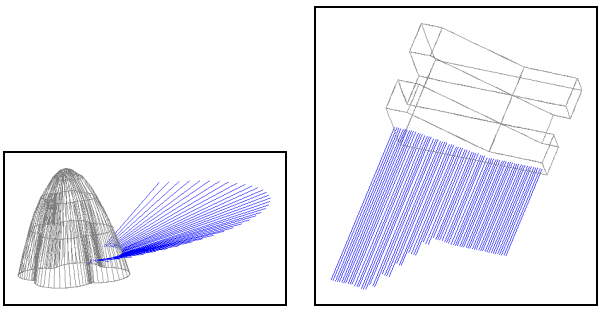

(a) (b)

Figure 8. (a) Viewpoint set with optimal orientation for a complex part. (b) Viewpoint set with optimal distance for a planar surface.

Reachability and the non-occlusion solutions. Until now, the viewpoints are found for the best accuracy condition. The next step in our strategy is to verify that the viewpoint position is reachable and is free from occlusion problem. For the reachability issue, we suppose that the part is in the center of a sphere, and that the viewpoints out of this sphere can be reached by the mechanical support of the camera. As the part is modeled according a *3D voxel model*, we can delimit the workspace by adding the model of other objects present in the scene. In the same way the system verifies that the displacement of the camera between viewpoints could be accomplished without collisions. When a collision problem is detected, the system solves it defining intermediate positions of displacement. For the verification of occlusion conditions, we insure that any object does not intersect the laser beam coming from the viewpoint position to the target surface. When an occlusion problem is detected, the system seeks for a new viewpoint by moving the old viewpoint in the parametric directions of the surface. The movement of the viewpoint is achieved by increasing the angle in the parametric directions until a valid viewpoint is found, that means a viewpoint that allows digitizing the desired surface portion. The new viewpoint will remain as near as possible to the normal direction to optimize the accuracy, but ensures the visibility of the region to be digitized. Figure 9 shows the digitalization viewpoints found for some surfaces that initially presented an occlusion problem.

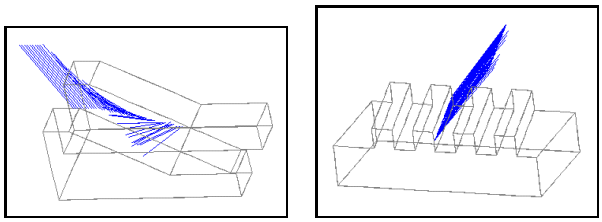

(a) (b)

Figure 9. Viewpoints set solution for surfaces exhibiting occlusion problem.

4.3. Estimation of 3D data accuracy

Once all the viewpoints have been located satisfying non-occlusion conditions, the strategy computes the accuracy of the 3D measured points as obtained from this set of viewpoints. If the result is satisfactory, this means that the 3D measured points have a better or the same accuracy as the specified one, then the solution is retained. Otherwise, a new set of viewpoints must be defined, and the algorithm is repeated from step 2: *Find the viewpoints set X*.

The accuracy of measured points in the case of an auto-synchronized camera is a function of the distance d between the camera and the part being digitized and the incident angles α and β of the laser beam. Thus, to estimate the accuracy of measured points, we must compute these parameters. Figure 10 illustrates some special configurations for

the determination of α and β parameters. The parameter d has been defined in a previous algorithm step.

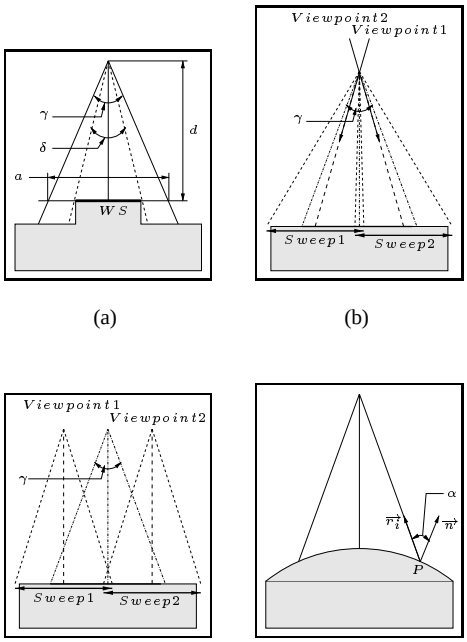

Figure 10. Evaluation of α and β parameters. (a) For a field of view greater than the surface. (b) Changing the viewpoint orientation to digitize the whole width of the surface. (c) Defining 2 new viewpoints to digitize the whole width of the surface. (d) Estimation on a complex surface.

Figure 10 (a) illustrates the case where the field of view of the range sensor is greater than the width of the surface to measure. The amplitude of the sweeping ray is computed from the field of view γ and the distance d. The width of the surface WS is obtained from the CAD model. As the resolution of the camera is well-known, that is the number of points in a sweep, the angle δ is calculated and so the incident angle of the sweep portion hitting the surface.

When the width of the measured surface is greater than the field of view of the range sensor, the strategy modifies the orientation of the camera (by using the mechanical support) in such a way that the incident angles α is always in $-35^\circ \leq \alpha \leq 35^\circ$ range (see Figure 10 (b)). If the maximum α value is reached and the width the surface has not been completely digitized, the trajectory is divided in two parallel trajectories as shown in Figure 10 (c). These computations are repeated iteratively until the whole surface is digitized.

In Figure 10 (d) we present the computation of the incident angle α in a curved surface. The point P where the ray touches the surface is calculated by using the 3D surface model. The normal on the surface at this point is obtained from the parametric NURBS surface. Finally the angle α is computed by developing the inner product of two vectors $\vec{r_i} \cdot \vec{n}$. When the surface is curved in the two parametric directions (u and v), the incident angles α and β are computed using the components of the normal in the direction of α and β variations.

Once the parameters d, α and β are known, the accuracy is computed as the sum of the dispersions introduced by each parameter, and obtained from the models developed in section 3.2.

If the accuracy of the measured points does not satisfy the specification, a new set of projected viewpoints must be defined. This new set consists of two parallel trajectories that use the old trajectory as an edge. The process is similar to the one illustrated in figure 10 (c).

Sometimes the required precision could not be obtained, particularly for surfaces having an occlusion problem. For such surface, the range sensor must have a great inclination to be able to scan the surface. When this happens, the system will indicate the regions that could not be digitized.

Although some parts in the algorithm could be costly in time, like the *3D voxel model* generation or the occlusion problem resolution, those processes are executed off-line. For the on-line portion, the system uses a registration process [20] to bring the CAD model and the set of computed viewpoints into the same cartesian coordinate system of the part.

5. Sensor placement strategy results

In the last section, we have described our strategy for automatically setting a sensor's placement for completely and accurately acquiring the geometry of a surface or of the complete part whenever possible. In this section, we present results of a sensing strategy for the complete digitalization of some parts. An auto-synchronized range sensor mounted on a coordinate measuring machine was used to acquire the 3D images.

Figure 11 (a) show the CAD model of a part. In Figure 11 (c), we look at the sensing strategy for a complete digitalization of a surface made of flat surfaces. Some surfaces of the part exhibited occlusion problem that was resolved. In Figure 11 (b), we show a range image of the part obtained by using the set of viewpoints. We can see that there are no missing regions of the part. We also digitize the part without the use of the sensor planning results from our strategy. We have evaluated the accuracy of those images by computing the distance between each measured point and the nearest point on the NURBS surface (CAD

model). The result was: for the image obtained without the strategy the mean distance was $0.073mm$ and for the image obtained with the strategy the mean distance was $0.048mm$. That means that we have improve the accuracy of measurements for about $25\mu m$, which is an important improvement for inspection task.

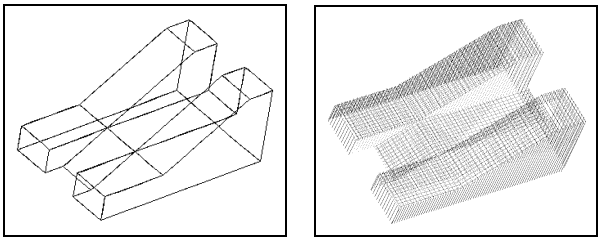

(a) (b)

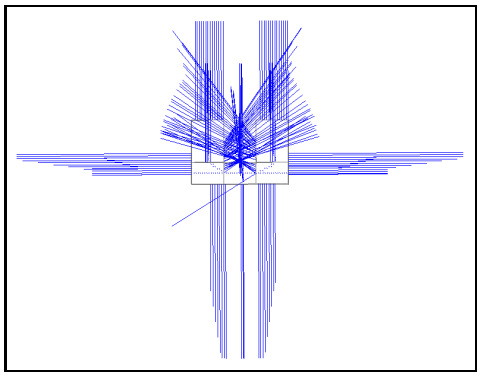

(c)

Figure 11. (a) CAD model of the part. (b) Synthesized range image. (c) Sensing strategy to digitize a simple part.

Figure 12 (a) show a CAD model of a part with complex surfaces. In Figure 12 (c), we illustrate the sensing strategy for the complete digitalization of this part and in Figure 12 (b), we show a range image of the part obtained by the set of viewpoints illustrated in Figure 12 (c). For this part we remark that the placement variation of viewpoints remains always near to the normal direction of the surfaces. The result of distance computation was: for the image obtained without the strategy the mean distance was $0.153mm$ and for the image obtained with the strategy the mean distance was $0.100mm$, so we improve the accuracy of measurements by about $53\mu m$

In Figure 13 (a) we show the 3D cloud of points obtained when we digitize a surface by using the set of viewpoints illustrated in Figure 9 (b). In the scanning process, point from

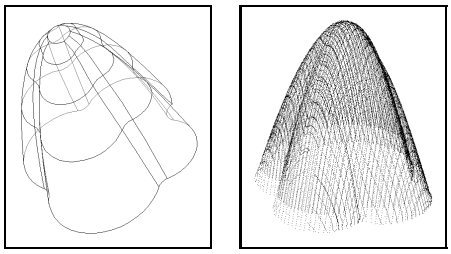

(a) (b)

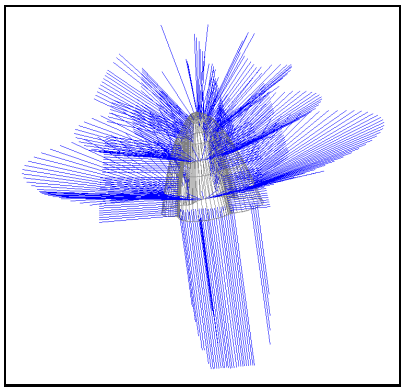

(c)

Figure 12. (a) CAD model of the part. (b) Synthesized range image. (c) Sensing strategy to digitize a complex part.

others surfaces are acquired because we can not control the field of view of the camera. But, as we know the exact placement of the camera, we are able to select the 3D points related to the surface of interest (Figure 13 (b)). Thus, the 3D data acquisition strategy permits to minimize overlap of the scans and to maximize accuracy of the data, so the 3D cloud of point will be optimal for inspection tasks.

6. Conclusion

We have presented an automated acquisition planning strategy to improve the accuracy of a cloud of measured 3D points. The strategy computes a set of viewpoints in order to obtain a complete and accurate 3D image of the part or selected surfaces in the part. The viewpoints are constrained to have the best accuracy conditions in the scanning process. For an auto-synchronized range sensor the accuracy of the 3D measured points is function of the distance to the part and of the incident angle with which the laser beam reaches the surface.

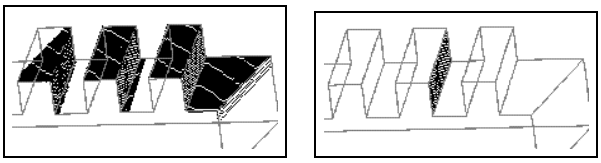

(a) (b)

Figure 13. Selection of the 3D points related to the surface of interest.

The system does not have any limitation in the geometry of parts to be scanned, meaning that it works as well with simple or complex parts. Knowledge of the exact position and orientation of the part and its CAD model are the only system requirements. The strategy can be easily adapted to use other kind of range sensors and mechanical supports. For that, the accuracy of the sensor has to be modelled.

The planning strategy allows us to digitize the whole part or the surfaces of interest with a specified accuracy. This property is important for inspection tasks, where most of the time we are interested in verifying the specification of just some few surfaces, because we will be able to have an accurate cloud of 3D measured points of the surface.

At present, the sequence of viewpoints for the scanning process is computed without any special computer configuration. Even if the acquisition planning is made off-line, it will be necessary to implement a method to optimally lay out the viewpoints in order to reduce the scanning time.

References

[1] C. Ben Amar, S. Perrin, H.T. Redarce and A. Jutard. Intégration d'un module vision dans un système de CAO-robotique: modélisation et aide au placement de capteurs. In *Congrès international de génie industriel la productivité dans un monde sans frontières*, pages 725–734, Montréal, Canada, octobre 18-20 1995.

[2] C.K. Cowan and P.D. Kovesi. Automatic sensor placement from vision-task requirements. *IEEE Transactions on Pattern Analysis and Machine Intelligence*, 10(5):pp. 407–416, May 1988.

[3] D. Papadopoulos-Orfanos and F. Schmitt. Automatic 3-D digitization using a laser rangefinder with a small field of view. In I. C. S. Press, editor, *Proceedings of the International Conference on Recent Advanced in 3-D Digital Imaging and Modeling, Ottawa, Canada*, pages 60–67, May 12-15 1997.

[4] E. Trucco, M. Diprima and V. Roberto. Visibility scripts for active feature-based inspection. *Pattern Recognition Letters*, 15:pp. 1151–1164, 1994.

[5] E. Trucco, M. Umasuthan, A.M. Wallace and V. Roberto. Model-based planning of optimal sensor placements for inspection. *IEEE Transactions on Robotics and Automation*, 13(2):pp. 182–194, April 1997.

[6] F. Blais, M. Rioux and J.A. Beraldin. Practical considerations for a design of a high precision 3-D laser scenner system. In *SPIE Optomechanical and Electro-Optical Design of Industrial Systems*, pages 225–246, Bellinghan, June 1988.

[7] F. Prieto, H.T. Redarce, R. Lepage and P. Boulanger. A non contact CAD based inspection system. In *Quality Control by Artificial Vision*, pages 133–138, Trois Rivières, Québec, Canada, 18-21 May 1999.

[8] H.T. Redarce, Y. Lucas, C. Ben Amar and S. Perrin. An integrated approach for programming vision inspection cells. *International Journal of Computer Integrated Manufacturing Systems*, 8(4):pp. 298–311, april 1995.

[9] J.A. Beraldin, L. Cournoyer, M. Rioux, F. Blais, S.F. El-Hakim and G. Godin. Object model creation from multiple range images: acquisition, calibration, model building and verification. In *Proceedings of the International Conference on Recent Advances in 3-D Digital Imaging and Modeling*, pages 326–333, Ottawa, Ont., May 12-15 1997.

[10] J.A. Beraldin, S.F. El-Hakim and F. Blais. Performance evaluation of three active vision systems built at the NRC. In *Proceedings of the Conference on Optical 3-D Measurement Techniques*, pages 352–362, Vienna, Austria, October 2-4 1995.

[11] K.A. Tarabanis, P.K. Allen and R.Y. Tsai. A survey of sensor planning in computer vision. *IEEE Transactions on Robotics and Automation*, 11(1):pp. 86–104, February 1995.

[12] K.A. Tarabanis, R.Y. Tsai and P.K. Allen. The MVP sensor planning system for robotic vision tasks. *IEEE Transactions on Robotics and Automation*, 11(1):pp. 72–85, February 1995.

[13] M. Rioux. Laser range finder based on synchronized scanners. *Applied Optics*, 23(21):3837–3844, November 1984.

[14] M. Rioux. Laser range finder based on syncronized scanners. In *SPIE Milestone Series, Optical Techniques for Industrial Inspection*, pages 142–149, Bellinghan, 1997.

[15] M. Rioux, G. Bechthold, D. Taylor, and M. Duggan. Design of a large depth of view three-dimensional camera for robot vision. *Optical Engineering*, 26(12):1245–1250, 1987.

[16] P.J. Besl and N.D. McKay. A method for registration of 3-D shapes. *IEEE Transactions on Pattern Analysis and Machine Intelligence*, 14(2):pp. 239–256, February 1992.

[17] R. Pito. A Sensor based solution to the next best view problem. In I. C. S. Press, editor, 13^{th} *International Conference on Pattern Recognition, Vienna, Austria*, pages A941–945, August 25-30 1996.

[18] R. Pito. *Automated surface acquisition using range cameras*. Ph.D. Dissertation: Computer and Information Science, University of Pennsylvania, GRASP Laboratory, Philadelphia, USA, 1997.

[19] T.S. Newman and A.K. Jain. A system for 3D CAD-based inspection using range images. *Pattern Recognition*, 28(10):pp. 1555–1574, 1995.

[20] V. Moron, P. Boulanger, P. Masuda and H.T. Redarce. Automatic inspection of industrial parts using 3-D optical range sensor. In *SPIE Proceedings, Videometrics IV*, volume 2598, pages 315–325, 1995.